J. Math. Biol.
DOI 10.1007/s00285-011-0455-z

Mathematical Biology

Stable and transient periodic oscillations in a mathematical model for CTL response to HTLV-I infection

John Lang · Michael Y. Li

Received: 11 March 2011

Abstract The cytotoxic T lymphocyte (CTL) response to the infection of $CD4^+$ T cells by human T cell leukemia virus type I (HTLV-I) has previously been modelled using standard response functions, with relatively simple dynamical outcomes. In this paper, we investigate the consequences of a more general CTL response and show that a sigmoidal response function gives rise to complex behaviours previously unobserved. Multiple equilibria are shown to exist and none of the equilibria is a global attractor during the chronic infection phase. Coexistence of local attractors with their own basin of attractions is the norm. In addition, both stable and unstable periodic oscillations can be created through Hopf bifurcations. We show that transient periodic oscillations occur when a saddle-type periodic solution exists. As a consequence, transient periodic oscillations can be robust and observable. Implications of our findings to the dynamics of CTL response to HTLV-I infections in vivo and pathogenesis of HAM/TSP are discussed.

Keywords HTLV-I infection · HAM/TSP · CTL response · Bi-stability · Stable periodic oscillations · Transient periodic oscillations · Hopf bifurcation

Mathematics Subject Classification (2000) 92D30 · 92D25

J. Lang (✉)
London School of Economics (LSE), London, UK
e-mail: j8lang@uwaterloo.ca

Present Address:
J. Lang
Department of Applied Mathematics, University of Waterloo,
Waterloo, Ontario N2L 3G1, Canada

M. Y. Li
Department of Mathematical and Statistical Sciences,
University of Alberta, Edmonton, AB T6G 2G1, Canada
e-mail: mli@math.ualberta.ca

Published online: 27 July 2011

1 Introduction

Human T cell leukemia virus type I (HTLV-I) is the etiologic agent for the HTLV-I associated myelopathy (HAM), a chronic inflammatory disease of the central nervous system, also called tropical spastic paraparesis (TSP) (Gout et al. 1990; Osame et al. 1990). HTLV-I infection can also lead to adult T cell leukemia (ATL) (Kubota et al. 2000; Gallo 2005). Approximately 20–40 million people are infected by HTLV-I worldwide. Endemic areas include the Caribbean, southern Japan, Central and South America, the Middle East, Melanesia, and equatorial Africa (Coffin et al. 1997). Most infected individuals remain lifelong asymptomatic carriers. Approximately 0.25–3.8% develop HAM/TSP and 2–3% of infected individuals develop ATL (Hollsberg and Hafler 1993; Bangham 2000).

In the peripheral blood, HTLV-I preferentially infects $CD4^+$ helper T cells (Richardson et al. 1990; Bangham 2000; Jacobson 2002). HTLV-I does not exist as free virions in vivo and infection of healthy $CD4^+$ T cells is achieved through cell-to-cell contact with infected $CD4^+$ T cells (Okochi et al. 1984; Bangham 2003). Infection also spreads vertically through mitosis of $CD4^+$ T cells that harbour HTLV-I provirus (Wattel et al. 1996). The vertical transmission allows for viral propagation without expression of the HTLV-I genome and explains the low rate of mutation in the HTLV-I genome (Wattel et al. 1996). It is known that the horizontal transmission of HTLV-I replication is active. The immune system reacts to HTLV-I infection with a strong cytotoxic T lymphocyte (CTL) response (Bangham 2000; Jacobson 2002). While CTL has a protective role by regulating the proviral load, evidence suggests that cytotoxicity of the CTL is ultimately responsible for the demyelination of the central nervous system resulting in HAM/TSP (Greten et al. 1998). The precise reason for the autoimmune response is unknown. One leading hypothesis is that the CTL response is reacting to cells in the CNS myelin which have become infected by HTLV-I (Bangham 2000; Jacobson 2002).

Understanding the pathogenesis of the HTLV-I within the host has important implications for the development of therapeutic measures and for the identification of risk factors for HAM/TSP. Mathematical models have been developed to capture the interaction in vivo among HTLV-I, its target cells, and the CTL immune response in order to explain the pathogenesis of HTLV-I-associated diseases (Wodarz et al. 1999; Nowak and May 2000; Wodarz and Bangham 2000; Gomez-Acevedo and Li 2002; Asquith and Bangham 2007; Gomez-Acevedo et al. 2010). The simplest mathematical model one can develop for this purpose consists of three compartments: healthy $CD4^+$ T cells x, proviral $CD4^+$ T cells y, and CTLs z. The model can be schematically shown using a transfer diagram as in Fig. 1.

As shown in Fig. 1, it is assumed in the model that healthy $CD4^+$ T cells are produced at a constant rate $\lambda > 0$. Compartments x, y, and z have turn-over rates μ_1, μ_2, and μ_3, respectively. The infection of healthy $CD4^+$ T cells is through direct cell-to-cell contact with a proviral $CD4^+$ T cell. This interaction is modeled by the mass action term βxy, where $\beta > 0$ is the transmission coefficient. The proviral $CD4^+$ T cells are constantly expressing the HTLV-I genome (Bangham 2000), and they are constantly subject to both antibody and CTL responses. We assume that a fraction σ of the newly infected $CD4^+$ T cells survive the antibody response. The loss of

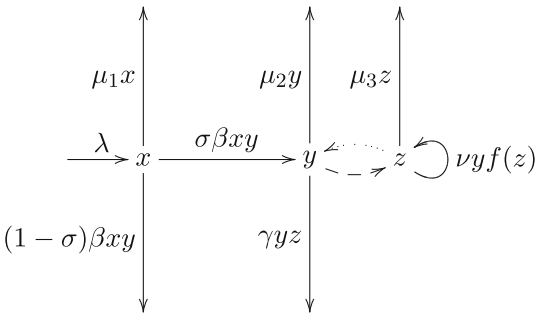

Fig. 1 Transfer diagram for the HTLV-I infection in vivo and the CTL response

proviral CD4$^+$ T cells due to CTL lysis is given by γyz. The term $\nu y f(z)$ represents the production of CTLs in response to HTLV-I, where $f(z)$ is the CTL response function. In the literature, CTL response function has taken a linear form $f(z) = z$ (Nowak and May 2000) or a density dependent form $f(z) = \frac{z}{z+a}$ with $a > 0$ (Wodarz et al. 1999; Gomez-Acevedo et al. 2010). These assumptions and the schematic diagram in Fig. 1 lead to the following system of differential equations for the model

$$\begin{aligned} \dot{x} &= \lambda - \beta xy - \mu_1 x \\ \dot{y} &= \sigma\beta xy - \gamma yz - \mu_2 y \\ \dot{z} &= \nu y f(z) - \mu_3 z. \end{aligned} \tag{1.1}$$

System (1.1) has three types of equilibria:

$$\begin{aligned} P_0 &= \left(\tfrac{\lambda}{\mu_1}, 0, 0\right), && \text{infection-free equilibrium,} \\ P_1 &= (\bar{x}, \bar{y}, 0), && \text{carrier equilibrium, and} \\ P^* &= (x^*, y^*, z^*), && \text{HAM/TSP equilibrium.} \end{aligned}$$

Here $\bar{x}, \bar{y}, x^*, y^*, z^*$ are all positive. At equilibrium P_0 the virus is cleared and all target CD4$^+$ T cells are healthy. At equilibrium P_1 the HTLV-I infection is chronic but the CTL response is absent, so are its cytotoxic effects on the central nervous system and the risk for developing HAM/TSP; this corresponds to the asymptomatic carrier state. At the positive equilibrium P^* the HTLV-I infection is chronic and there is a persistent CTL response and constant cytotoxic effect on the central nervous system; this corresponds to the HAM/TSP state. It is shown in Gomez-Acevedo et al. (2010) that, for $f(z) = \frac{z}{z+a}$, the final outcomes of the system are determined by values of two threshold parameters,

$$R_0 = \frac{\lambda\sigma\beta}{\mu_1\mu_2}, \quad \text{and} \quad R_1 = \frac{\lambda\sigma\beta\nu}{\mu_2(\mu_1\nu + \beta\mu_3)}, \tag{1.2}$$

and they are called the basic reproduction numbers for HTLV-I infection and the CTL response, respectively. The global dynamics of system (1.1) is completely determined in Gomez-Acevedo et al. (2010). Their results can be summarized in Table 1.

Table 1 Global dynamics of model (1.1) for $f(z) = \frac{z}{z+a}$ (Gomez-Acevedo et al. 2010)

Threshold value	Equilibria		
	P_0	P_1	P^*
$R_1 < R_0 < 1$	GAS[a]	DNE[b]	DNE
$R_1 < 1 < R_0$	Unstable	GAS	DNE
$1 < R_1 < R_0$	Unstable	Unstable	GAS

[a] Globally Asymptotically Stable. By this we mean asymptotically stable within the interior of Γ, see (2.1)
[b] Does not exist

Wodarz et al. (1999) considered the following model that includes mitotic divisions in both healthy and proviral CD4$^+$ T cells:

$$\begin{aligned} \dot{x} &= (\lambda + rx)\left(1 - \frac{x+y}{k}\right) - \beta xy - \mu_1 x \\ \dot{y} &= \beta xy + sy\left(1 - \frac{z+y}{k}\right) - \gamma yz - \mu_2 y \\ \dot{z} &= \nu \frac{yz}{z+1} - \mu_3 z. \end{aligned} \tag{1.3}$$

Model (1.3) not only has equilibria as outcomes; it can have stable periodic oscillations in certain parameter regions, which are not present in the models of Gomez-Acevedo et al. (2010). The existence of stable periodic oscillations is used in Wodarz et al. (1999) to explain patient data that shows treatment-induced transient oscillations. In a simpler version of model (1.3), Wodarz and Bangham (2000) showed that model (1.3) can possess a bistability phenomenon: both P_0 and P^* exist and are both stable when R_0 is below threshold 1. In this case, the outcome of system is critically dependent on the initial conditions. This is also related to the backward bifurcation observed in a simple HTLV-I model in Gomez-Acevedo and Li (2005).

HTLV-I specific CTL response typically occurs after a time lag from weeks to months after seroconversion. To better describe this lagged response during the early stage of the infection when z is small, as well as the saturation effect when z is large, we propose to approximate the response function using a sigmoidal function of form

$$f(z) = \frac{z^n}{z^n + a}, \quad a > 0, \ n \geq 2. \tag{1.4}$$

Functions of this form are commonly used for modeling of enzyme kinetics as well as in the ecological modeling literature. Such a response function when $n = 2$ was used in a model for general autoimmune disorders in Iwami et al. (2007). The objective of our study is to investigate whether sustained oscillations and bistability in model (1.1) can be the result of immune response alone, without mitosis. Our analysis of model (1.1) with general response functions in (1.4) reveals a wide array of possible outcomes of the dynamics, many of which have not been observed before or are distinct from those observed in earlier models. Of particular interest are the following new results:

(1) The carrier equilibrium P_1 is always asymptotically stable when $R_0 > 1$. This finding is different from those in Wodarz and Bangham (2000) and Gomez-Acevedo et al. (2010), where P_1 can lose stability when the value of R_0 is sufficiently large. Our result can better explain the fact that most of HTLV-I infected people remain as life-long asymptomatic carriers.

(2) Bistability. We show that, for a large region of parameter values, it is possible for the carrier equilibrium P_1 and a HAM/TSP equilibrium P^* to coexist and both be stable, when R_0 is above threshold 1. In this case, a solution remains close to the stable carrier equilibrium until perturbations force it to cross into the basin of attraction of the HAM/TSP equilibrium. This provides an explanation why an infected person can remain asymptomatic for a long time before developing HAM/TSP.

(3) Existence of stable periodic oscillations. We show that stable periodic solutions exist through supercritical Hopf bifurcations near the HAM/TSP equilibrium. Stable periodic solutions have also been shown to exist in Wodarz and Bangham (2000) in a model with both CTL response and mitosis of proviral target cells. Our result demonstrates that stable periodic solutions can be the result of CTL response alone without mitosis. This is significant for dynamics of immune responses to infection of viruses such as HIV-I or HBV, for which mitosis may not be as important for viral replication. Because the carrier equilibrium P_1 is always stable when HTLV-I infection is chronic, it is possible for the coexistence of a stable equilibrium P_1 and a stable periodic solution. This suggests that when HAM/TSP develops, the proviral load can either approach an equilibrium level or appear as sustained oscillations.

(4) Existence of transient periodic oscillations. We show that subcritical Hopf bifurcations can also occur in model (1.1) for a large range of parameter values. The resulting periodic solutions are of saddle type. They are unstable and thus transient. Nonetheless, they are robust with respect to small perturbations because of the saddle property and thus observable. These robust but transient periodic solutions are not commonly observed in mathematical models in biological context and have not received much research attention. Biological implications of their existence to HTLV-I infection and development of HAM/TSP need to be further investigated. HAM/TSP patients undergoing treatments are known to exhibit episodes of transient oscillations in their proviral loads and CTL frequency (Wodarz et al. 1999). Large-amplitude transient oscillations have consistently been observed in equine infectious anemia virus (EIAV) infection data (Leroux et al. 2004). Our results suggest that the lagged CTL response may be responsible for the occurrence of transient oscillations.

(5) Hysteresis. Bistability in cases (2) and (3) leads to hysteresis behaviours; as a parameter is increased or decreased, the system may follow two different branches of stable equilibria. In our case, it is possible that the system follows a branch of stable equilibria as a parameter decreases and follows a branch of stable periodic solutions as the parameter increases, resulting in completely different dynamical behaviours (see Fig. 3b). Hysteresis behaviours have significant implications for potential treatment and intervention measures.

In Sects. 2–4, we present mathematical and numerical evidence for our findings. Further discussions are given in Sect. 5. Mathematical proofs are provided in the Appendix.

2 Equilibria and bistability

Model (1.1) will be investigated in the following bounded feasible region

$$\Gamma = \left\{(x, y, z) \in \mathbb{R}^3_+ : x \le \frac{\lambda}{\mu_1}, x + y \le \frac{\lambda}{\bar{m}}, z \le \frac{\lambda\nu}{\bar{m}\mu_3}\right\}, \tag{2.1}$$

where $\bar{m} = \min\{\mu_1, \mu_2\}$. It can be shown that all solutions of (1.1) eventually enter Γ, and that Γ is positively invariant with respect to system (1.1).

From equilibrium equations

$$\begin{aligned} \lambda - \beta xy - \mu_1 x &= 0, \\ \sigma\beta xy - \gamma yz - \mu_2 y &= 0, \\ \nu y f(z) - \mu_3 z &= 0, \end{aligned} \tag{2.2}$$

we know that the infection-free equilibrium $P_0 = (\lambda/\mu_1, 0, 0)$ always exists. The carrier equilibrium $P_1 = (\bar{x}, \bar{y}, 0)$ satisfies equations

$$\lambda - \beta\bar{x}\bar{y} - \mu_1\bar{x} = 0, \quad \sigma\beta\bar{x} = \mu_2,$$

and it exists if and only if $R_0 = \frac{\lambda\sigma\beta}{\mu_1\mu_2} > 1$. For a positive (HAM/TSP) equilibrium $P^* = (x^*, y^*, z^*)$, $x^*, y^*, z^* > 0$, we can show that z^* is a positive solution of the equation

$$f(z) = h(z), \tag{2.3}$$

where $f(z)$ is the response function and

$$h(z) = \frac{\beta\mu_3}{\nu}\frac{\mu_2 z + \gamma z^2}{\lambda\sigma\beta - \mu_1\mu_2 - \mu_1\gamma z}.$$

Graphically, a solution z^* of Eq. (2.3) corresponds to an intersection in the first quadrant of graphs of $f(z)$ and $h(z)$. For $0 \le z \le \frac{\mu_2}{\gamma}(R_0 - 1)$, $h(z) \ge 0$ and is concave up, while $f(z)$ can change its concavity when $n \ge 2$, their graphs can have no, exactly one, or two intersections, as we demonstrate in Fig. 2. As a consequence, when $R_0 > 1$, there can be no, exactly one, or two HAM/TSP equilibria. We summarize these results in the next theorem. Detailed proof will be given in the Appendix.

Let

$$\begin{aligned} g(z) = {} & \beta\mu_3\gamma z^{n+1} + (\nu\mu_1\gamma + \beta\mu_2\mu_3)z^n - \nu(\lambda\sigma\beta - \mu_1\mu_2)z^{n-1} \\ & + a\beta\mu_3\gamma z + a\beta\mu_2\mu_3, \end{aligned}$$

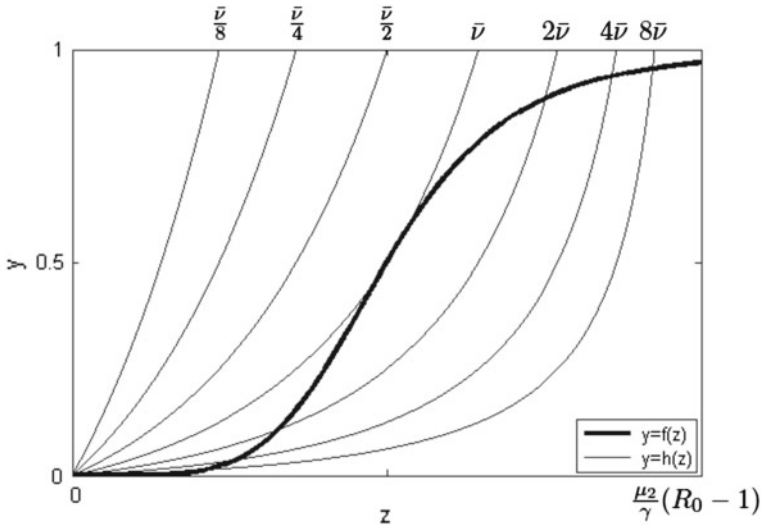

Fig. 2 Intersections of graphs of $f(z)$ and $h(z)$

and

$$m = \min\left\{g(z) : 0 \le z \le \frac{\mu_2}{\gamma}(R_0 - 1)\right\}.$$

Theorem 2.1 (a) *The infection-free equilibrium* $P_0 = (\tilde{x}, 0, 0) = \left(\frac{\lambda}{\mu_1}, 0, 0\right)$ *always exists.*

(b) *The carrier equilibrium*

$$P_1 = (\bar{x}, \bar{y}, 0) = \left(\frac{\mu_2}{\sigma\beta}, \frac{\lambda\sigma\beta - \mu_1\mu_2}{\beta\mu_2}, 0\right)$$

exists if and only if $R_0 > 1$.

(c) *If* $R_0 > 1$ *and if* $m > 0$, *then there is no HAM/TSP equilibrium.*

(d) *If* $R_0 > 1$ *and if* $m = 0$, *then there is exactly one HAM/TSP equilibrium*

$$P^* = (x^*, y^*, z^*), \quad x^*, y^*, z^* > 0.$$

(e) *If* $R_0 > 1$ *and if* $m < 0$, *then there are two HAM/TSP equilibria,*

$$P^* = (x^*, y^*, z^*) \quad \textit{and} \quad P^{**} = (x^{**}, y^{**}, z^{**}),$$

where $z^{**} > z^* > 0$.

Stability results of equilibria are summarized in the following theorem, whose proof is given in the Appendix.

Theorem 2.2 (a) *If $R_0 \leq 1$, then the infection-free equilibrium P_0 is globally asymptotically stable in Γ, and the virus is cleared. If $R_0 > 1$, P_0 is unstable and the HTLV-I infection becomes chronic.*

(b) *If $R_0 > 1$, then the carrier equilibrium P_1 comes to exist and is always locally asymptotically stable.*

From Theorem 2.2, we know that the basic reproduction number R_0 for asymptomatic carriers and HAM/TSP patients should be above the threshold 1. The fact that carrier equilibrium P_1 remains asymptotically stable implies that an infected person tends to remain as a carrier for a long time. This offers an explanation why HTLV-I infection has a long latent period and why most of HTLV-I infected people remain as life-long asymptomatic carriers.

The phenomenon that carrier equilibrium P_1 remains asymptotically stable for $R_0 > 1$ opens up opportunities for bistability in the system when HTLV-I infection is chronic. We show through numerical simulations that, for large range of parameter values, a stable HAM/TSP equilibrium P^* or a stable periodic solution can coexist with P_1 (see Figs. 3, 6). An important implication of bistability is that outcomes of the system critically depends on the initial conditions. It is highly likely in such a situation that a solution remains in the basin of attraction of the carrier equilibrium and then is forced by system perturbations into the basin of attraction of the stable HAM/TSP equilibrium. This provides a plausible mechanism for the development of HAM/TSP after a long incubation period.

3 Stable oscillations

As proved in Theorem 2.1 and shown in Fig. 2, when parameters vary, system (1.1) may change from having no HAM/TSP equilibrium to have two branches of HAM/TSP equilibria P^* and P^{**}. We show through numerical simulations that stability change may occur to the branch of P^{**}, leading to a Hopf bifurcation. We also note that, as parameters increase, the branch of HAM/TSP equilibrium P^{**} can change from stable to unstable or vice versa, and the Hopf bifurcation can be either supercritical or subcritical. Correspondingly, the resulting periodic solutions from the Hopf bifurcation can be either stable or unstable. In this section, we show numerical evidence for stable periodic solutions. In the next section, we discuss unstable periodic solutions.

Bifurcation diagrams and numerical solutions to (1.1) are generated in MATLAB. Stable and unstable periodic solutions are detected using XPPAUTO. Scales used in figures are arbitrary for ease of display. We note that although the simulations shown below are for the case $n = 2$, similar results can be observed for integer values of $n \geq 2$. We use a vector $\mathbf{p}$ to include all the parameters in (1.1).

$$\mathbf{p} = (\lambda, \beta, \sigma, \gamma, \nu, a, \mu_1, \mu_2, \mu_3).$$

Consider parameter values given by

$$\mathbf{p} = (2, 1, 1, 1.99, 3.85, 0.45, 1, 1, 0.5). \tag{3.1}$$

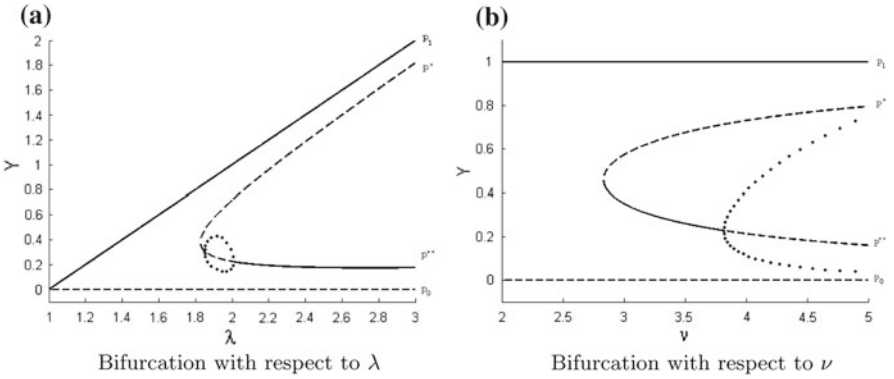

Fig. 3 Supercritical Hopf bifurcation with **p** as in (3.1). *Solid lines* indicate stable equilibria, *dash lines* unstable equilibria, and *dotted lines* stable periodic solutions

We have observed a super-critical Hopf bifurcation when we change each of parameters. We include representative bifurcation diagrams with respect to parameters λ and ν in Fig. 3. Solid lines indicate stable equilibria, dash lines indicate unstable equilibria, and dotted lines are for stable periodic solutions.

From bifurcation diagrams in Fig. 3, we see that supercritical Hopf bifurcations occur when we vary parameter λ or ν. In both cases, a stable periodic solution persists for a large range of the bifurcation parameter. However, there is a distinct difference in the nature of the λ and ν Hopf bifurcations: the Hopf branch with respect to λ is bounded and eventually vanishes as λ increases; in contrast, the Hopf branch with respect to ν persists as ν increases. This difference can be further demonstrated in two-parameter bifurcation analysis. In Fig. 4, stability region of the HAM/TSP equilibrium P^{**} is shown in the $\lambda\mu$-parameter plane. The dark region contains values of (λ, ν) for which P^{**} is stable, while the light region corresponds to parameter values for which P^{**} is unstable. If we let λ vary along a horizontal line across the light region, P^{**} loses its stability when the line first crosses from the dark region into the light region, creating the Hopf bifurcation. When the line exists the light region into the dark region on the right, P^{**} regains its stability, a backward Hopf bifurcation occurs, and the Hopf branch terminates. In a similar fashion, if we let ν vary along a vertical line through the light region, Hopf bifurcation only occurs once and the Hopf branch persists.

From the bifurcation diagrams in Fig. 3, we also see that bistability occurs in two different forms: a stable carrier equilibrium P_1 and a stable HAM/TSP equilibrium P^{**} coexist, or a stable P_1 and a stable periodic solution near P^{**} coexist. In these situations, different initial conditions may lead to different outcomes, for the same set of parameters. We demonstrate these phenomena in Fig. 5. We fix the parameter vector **p** as in (3.1). We select two set of initial conditions which are very close to each other:

$$(x(0), y(0), z(0)) = (2, 0.5, 0.5) \quad \text{and} \tag{3.2a}$$

$$(x(0), y(0), z(0)) = (2, 0.25, 0.5) \approx P^{**} \tag{3.2b}$$

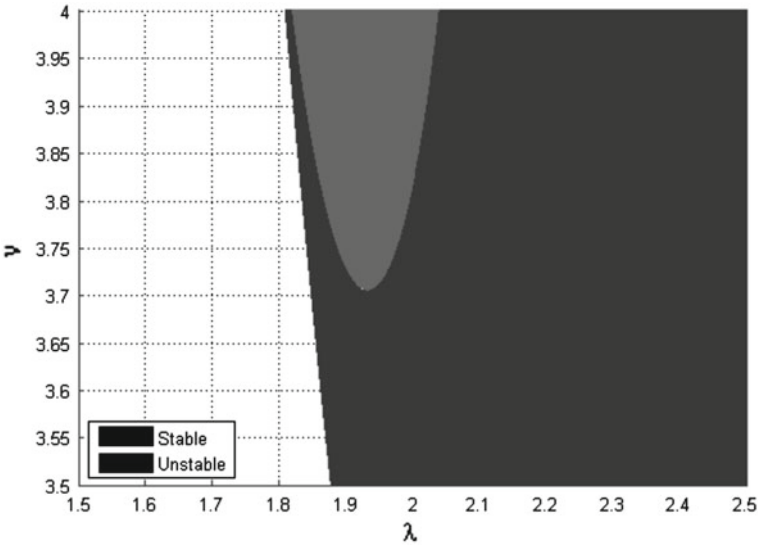

Fig. 4 Region of stability of P^{**} in the $\lambda\nu$-plane

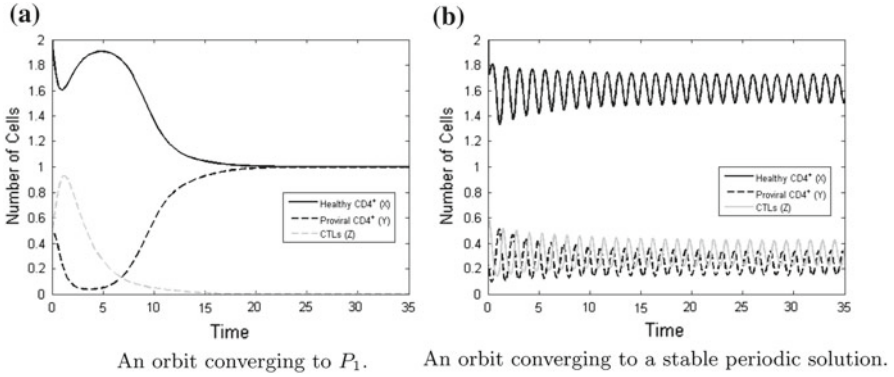

Fig. 5 Two orbits showing bistability with **p** as in (3.1)

As shown in Fig. 5, one solution converges to the carrier equilibrium P_1 while the other converges to the stable periodic orbit.

4 Transient oscillations that are robust

Consider the parameter vector

$$\mathbf{p} = (0.25, 1, 0.5, 4, 1.25, 0.01, 0.01, 0.1, 1). \tag{4.1}$$

A different kind of Hopf bifurcation occurs when the parameters are varied from this value of **p**. We show the bifurcation diagrams for parameters λ and ν in Fig. 6, and

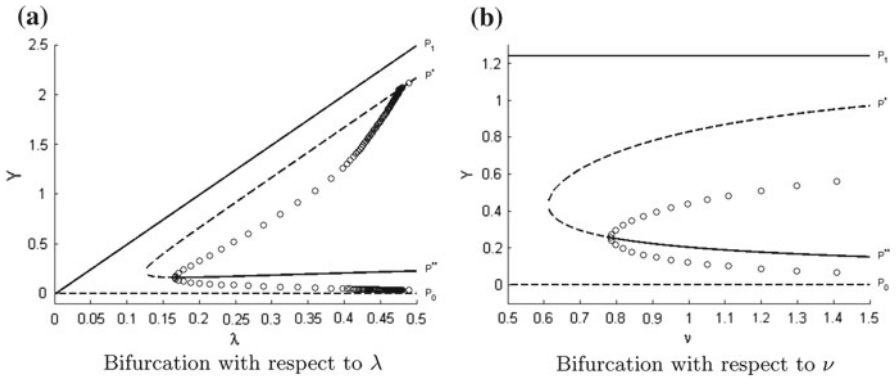

Fig. 6 Subcritical Hopf bifurcation with **p** as in (4.1). *Solid lines* indicate stable equilibria, *dashed lines* unstable equilibria, and *circles* indicate unstable periodic solutions

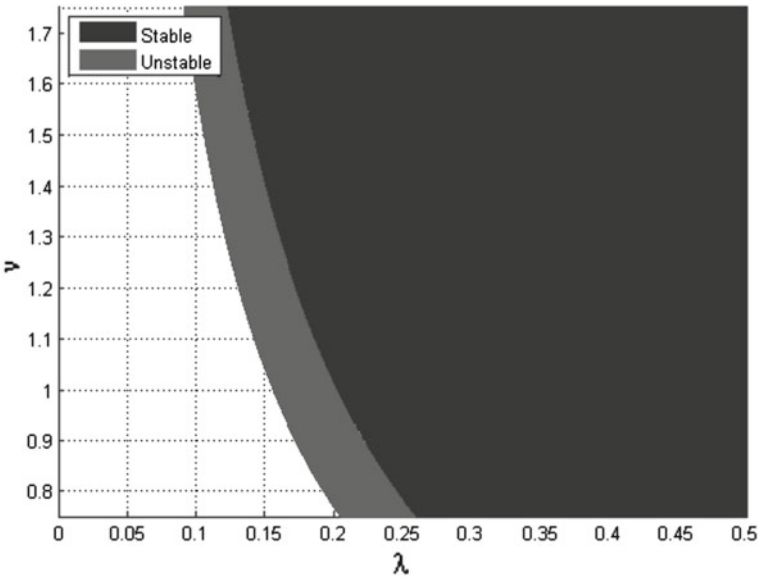

Fig. 7 Stability region of P^{**} in the $\lambda\nu$ plane, with **p** as in (4.1)

the corresponding two-parameter bifurcation analysis in Fig. 7. Similar bifurcation diagrams are observed when other parameters are varied.

In Fig. 6, as the parameter λ or ν is increased, stability of the lower branch of the HAM/TSP equilibrium P^{**} changes from unstable (dashed line) to stable (solid line), and a branch of unstable periodic solutions (circles) are created. This is called a subcritical Hopf bifurcation, a phenomenon often ignored in biological models, largely due to a misconception that an unstable periodic solution is not detectable or observable.

We show in Figs. 8 and 9 that these unstable periodic solutions are robust and observable, and can be easily detected in numerical simulations. In Fig. 8, solutions track a periodic orbit for sometime before converging to one of the stable equilibria.

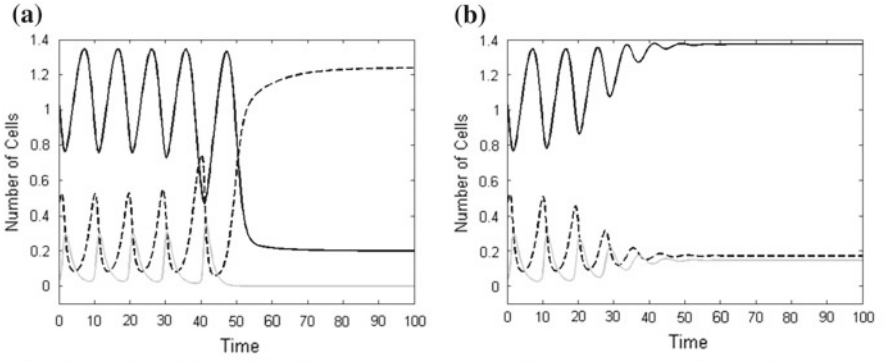

The orbit with initial condition (4.2a) converges to the carrier equilibrium P_1

The orbit with initial condition (4.2b) converges to the HAM/TSP equilibrium P^{**}

Fig. 8 Two transient periodic oscillations converging to different equilibria with **p** as in (4.1)

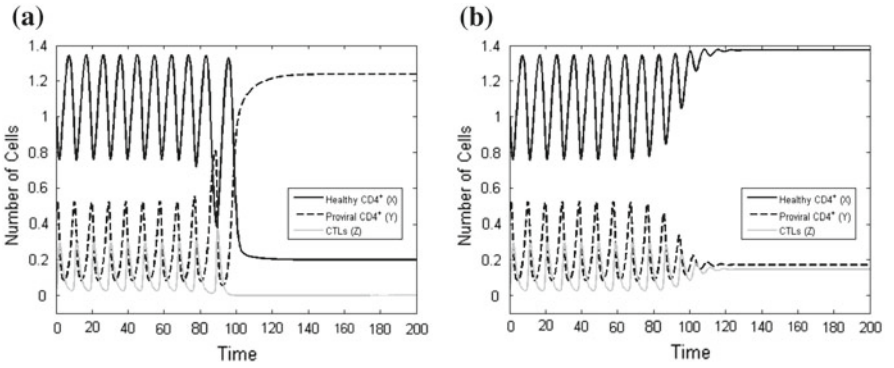

The orbit with initial conditions (4.3a) converges to the carrier equilibrium P_1

The orbit with initial conditions (4.3b) converges the HAM/TSP equilibrium P^{**}

Fig. 9 Long-lasting transient periodic solutions with **p** as in (4.1)

These oscillations are different from damped oscillations, since, for the same set of parameter values, by choosing different initial conditions, we can have solutions that track the unstable periodic solution for as long as we wish (see Fig. 9). These oscillations are also transient since they are all tracking an unstable periodic solution. The mathematical explanation for these robust transient oscillations is the following: the unstable periodic solution from the Hopf bifurcation is of a saddle type; it has a Floquet multiplier greater than 1 and another less than 1. As a result, the periodic orbit has a two-dimensional center-unstable manifold and a two-dimensional center-stable manifold. Solutions starting near the center-stable manifold will be quickly attracted to a neighborhood of the periodic solution, stay a long time in the neighborhood while behaving like a periodic solution, then leave the neighborhood along the center-unstable manifold. To observe such a saddle-type periodic orbit, one need only choose initial conditions close to the center-stable manifold which may contain points that are far from the periodic orbit itself.

Given the existence of bistable equilibria P_1 and P^{**}, it is not hard to see that the unstable periodic solution is located on the boundary of basins of attractions of P_1 and P^{**}. Naturally, one expects that the transient oscillations could converge either to P_1 or to P^{**}. Indeed, in Fig. 8, we use the parameter vector in (4.1) and choose two initial conditions that are close to each other:

$$(x(0), y(0), z(0)) = (0.83040, 0.51130, 0.14677), \quad \text{and} \tag{4.2a}$$

$$(x(0), y(0), z(0)) = (0.83042, 0.51124, 0.14675). \tag{4.2b}$$

The two resulting transient periodic oscillations converge to two different equilibria.

In Fig. 9 we use the parameter vector in (4.1) and choose a different set of initial conditions:

$$(x(0), y(0), z(0)) = (0.8240345, 0.2502873, 0.1107864), \quad \text{and} \tag{4.3a}$$

$$(x(0), y(0), z(0)) = (0.8240676, 0.2420150, 0.1108380). \tag{4.3b}$$

We observe that the two transient periodic oscillations converge to different equilibria as in Fig. 8. Furthermore, both oscillations in Fig. 9 appear periodic for much longer a time than those in Fig. 8. In fact, by selecting initial conditions, we can produce transient periodic oscillations that last for any desired length of time.

5 Discussions

In this paper, using a sigmoidal response function to model the CTL response to the human T cell leukaemia/lymphoma virus type I (HTLV-I) infection in vivo, we have shown that that the dynamic interactions between the immune response and viral infections can be very complex and multi-faceted. The outcomes of our model (1.1) can be summarized into four main types: bistability, stable periodic solutions, unstable periodic solutions, and hysteresis. Our model analysis have revealed new dynamics that have not been previously observed for this type of models. In comparison to the study in Wodarz et al. (1999), we have intentionally neglected the effect of mitosis of the $CD4^+$ target cells, and we are able to show that Hopf bifurcations and complex behaviours can be the result of interplay between CTL response and the viral infection, whether or not mitosis is playing a role in the process. We comment that our findings are based on the assumption that viral transmission is through cell-to-cell contact and virological synapse. Recent research has shown that this route of transmission also occurs in the infection of other retroviruses including HIV-I (Feldmann and Schwartz 2010; Hübner et al. 2009). In this light, our findings may have important implications for modeling immune response to infections from viruses such as HIV-I, HCV and HBV, where mitosis may not play as an important role as believed in HTLV-I infection.

5.1 Bistability and HAM/TSP development

Previously documented bistability in these type of models (Wodarz and Bangham 2000) results from the coexistence of a stable infection-free equilibrium and a stable

HAM/TSP equilibrium when the basic reproduction number R_0 is below the threshold of 1. We have shown in our model that, when HTLV-I infection is chronic ($R_0 > 1$), the carrier equilibrium remains stable and can coexist with a stable HAM/TSP steady-state either in the form of equilibrium or in the form of periodic oscillations. This is a different and more general phenomenon than the bistability in Wodarz et al. (1999). Our results provide new insights for the long incubation period and development of HAM/TSP. Since the HTLV-I infection is life-long, we may assume that infected individuals have $R_0 > 1$. In such a case, if the initial infection is in the basin of attraction of the stable carrier equilibrium P_1, then the individual will remain a carrier for a long period of time. Because of the coexistence of a stable HAM/TSP steady state, perturbations to the system that might result from subsequent exposure to HTLV-I or physiological changes can cause the trajectory of the system to move into the basin of attraction of the HAM/TSP steady state, resulting in the development of HAM/TSP. How close the trajectory is to the boundary of the two basins of attraction determines how easy it is for the HAM/TSP to develop. Compared to previous modelling studies of HTLV-I and HAM/TSP, our result reveals that it is possible to change the course of HAM/TSP development through perturbations of a trajectory rather than to the physiological or immunological parameters. Our result implies that the initial dosage of HTLV-I, subsequent exposure to HTLV-I, and routes of HTLV-I infection can all be important risk factors of HAM/TSP development. This is supported by clinical HAM/TSP studies using animal models. Kato et al. (1998) has demonstrated that adult rats orally inoculated with HTLV-1-producing cells develop a persistent HTLV-1 infection with no humoral and cellular immune responses, while adult rats intravenously or intraperitoneally inoculated with the same cell line developed significant CTL response specific to HTLV-1. Osame et al. (1990) has shown that HTLV-I infection through blood transfusion is positively correlated with higher numbers of HAM/TSP patients. Seto et al. (1995) has shown that chronic progressive myeloneuropathy can be developed in rats intraperitoneally inoculated with HTLV-I producing cells, after a long incubation period, and that a high dose of inoculation can significantly accelerate the disease onset.

5.2 Transient and robust periodic oscillations

Another significant new phenomenon our study has revealed is the existence of transient periodic oscillations that are robust and observable. These unstable periodic solutions are created through a subcritical Hopf bifurcation when parameter values are changed (Figs. 6, 7). A surprising property of these periodic solutions is that they are of saddle type, namely, they have both stable and unstable manifolds. In the terminology of nonlinear dynamics, the corresponding fixed point of the associated Poincaré map is a saddle with one-dimensional stable manifold and one-dimensional unstable manifold. This property has created many interesting features for this type of oscillations: (1) they are transient since the periodic solution is unstable, and they will converge to one of the stable equilibria as time goes on (Fig. 8); (2) they are robust with respect to small perturbations of parameters and initial conditions due to the normal hyperbolicity of the periodic solutions, for the same reason that a saddle-type fixed

point is robust with respect to small perturbations; (3) they are easily observable and detectable in model simulations. This is because nearby solutions tend to stay close to and track the periodic solution for some time, and hence appear as periodic oscillations (Figs. 8, 9). We also note that these "nearby" solutions can be produced by choosing initial conditions close to the center-stable manifold of the periodic solution, not necessarily close to the periodic solution itself; and (4) for the same set of parameter values, these transient oscillations may last for a variable length of time depending on how close the initial condition is from the center-stable manifold (Figs. 8, 9). We comment that subcritical Hopf bifurcations have received little attention in biological modelling literature, likely due to a misconception that unstable periodic solutions are not detectable nor observable. Another reason for the neglect of subcritical Hopf bifurcations is an often misguided belief that they are supercritical Hopf bifurcations with a reverse change of parameters. Our discovery that saddle-type periodic solutions can be created through a Hopf bifurcation in a biological model demonstrates that these common beliefs are faulty, and biological significance of the transient and robust periodic solutions ought to be further explored.

Some HTLV-I data has shown transient periodic oscillations after treatment (Wodarz et al. 1999). Clinical data from other viral infections such as EIAV, a retrovirus related to HIV, also show episodes of transient and sustained oscillations in both viral load and CTL abundance (Leroux et al. 2004). In the study of Wodarz et al. (1999), the route to periodic oscillations is described as a switching of drug therapies which perturbs model parameters back and forth, creating and then destroying a stable periodic solution within a finite time. Our result offers a different explanation: therapies can produce small perturbations to the orbit, and switch it to the neighborhood of an unstable periodic solution and produce transient periodic oscillations.

5.3 Treatment implications of hysteresis behaviours

Currently, there is no established treatment program for HAM/TSP. Several agents including corticosteroids, plasmapheresis, danazol, pentoxifylline, and interferon have been reported to show short-term clinical improvements, but none have been conclusively shown to alter the long-term disability of HAM/TSP (Oh and Jacobson 2008). Clinical studies suggest that interferon-α provides benefits over short periods. The long-term benefits of interferon, however, has not been established. Complicated dynamics in our model, especially when hysteric behaviours are present, may provide an explanation for why long-term benefits of interferon treatment are hard to achieve. HAM/TSP in our model is represented by solutions lying in the basin of attraction of the stable HAM/TSP equilibrium P^{**}, while ACs are represented by solutions staying in the basin of attraction of the stable AC equilibrium P_1. Interferon-α can interfere with viral activities and viral entry of cells and hence reduce the transmission coefficient β. For interferon-α treatments to be effective, it has to shift a solution from the basin of attraction of the HAP/TSP equilibrium P^{**} into that of the AC equilibrium P_1. Once this is achieved, the treatment must then be terminated in a continuous fashion to ensure that the solution will remain in the basin of attraction of P_1, as shown in Fig. 10a. Discontinuing the treatment in a gradual fashion is critically important, since

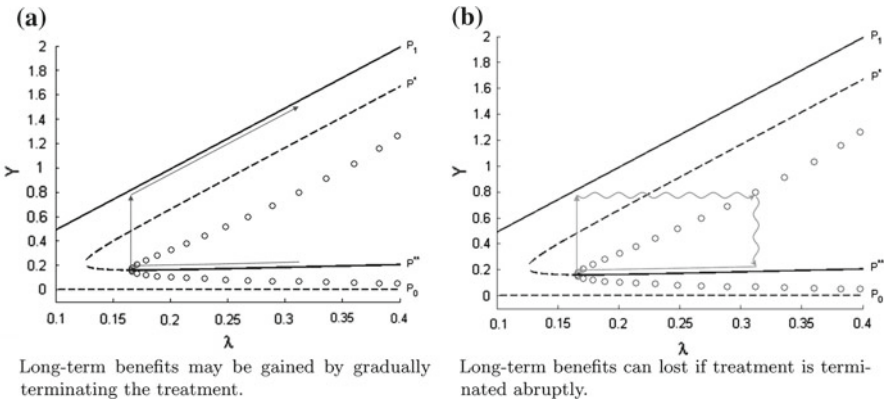

Fig. 10 Hysteresis behaviours that may impact treatments of HAM/TSP

a rapid change in parameters may result in the solution passing back into the basin of attraction of the HAM/TSP equilibrium, with short-term gains of the treatment completely lost (see Fig. 10b).

Acknowledgments The research is supported in part by grants from the Natural Science and Engineering Research Council (NSERC) of Canada and Canada Foundation of Innovation (CFI). MYL acknowledges the support of NCE-MITACS project "Transmission Dynamics and Spatial Spread of Infectious Diseases: Modelling, Prediction and Control." JL acknowledges the support of an NSERC Postgraduate Scholarship.

Appendix: Proofs

Feasible region Γ and its positive invariance

It can be verified from (1.1) that $\mathbb{R}^3_+$ is positively invariant. Since populations of cells are non-negative quantities, we restrict any further analysis of this model to $\mathbb{R}^3_+$. From the first equation of (1.1) we get $\dot{x} \le \lambda - \mu_1 x$ and this implies $x(t) \le \frac{\lambda}{\mu_1}$ for all $t \ge 0$ if $x(0) \le \frac{\lambda}{\mu_1}$ and

$$\limsup_{t\to\infty} x(t) \le \frac{\lambda}{\mu_1}.$$

A similar treatment of $x(t) + y(t)$ allows us to show

$$x(t) + y(t) \le \frac{\lambda}{\bar{m}} \quad \text{for } t \ge 0 \quad \text{if } x(0) + y(0) \le \frac{\lambda}{\bar{m}},$$

and

$$\limsup_{t\to\infty} x(t) + y(t) \le \frac{\lambda}{\bar{m}},$$

where $\bar{m} = \min\{\mu_1, \mu_2\}$. The bounds on x and $x + y$ and a similar argument for the z equation allow us to show $z(t) \leq \lambda\nu/\bar{m}\mu_3$ for $t \geq 0$ if $z(0) \leq \lambda\nu/\bar{m}\mu_3$, and

$$\limsup_{t\to\infty} z(t) \leq \frac{\lambda\nu}{\bar{m}\mu_3}.$$

These relations establish the boundedness and positive invariance of the feasible region Γ.

Theorem 2.1: Number of HAM/TSP equilibria

From equilibrium equation (2.2) we know that a HAM/TSP equilibrium with nonzero z must satisfy

$$x = \frac{\mu_2 + \gamma z}{\sigma\beta} \quad \text{and}$$
$$y = \frac{\lambda\sigma\beta - \mu_1\mu_2 - \mu_1\gamma z}{\beta\mu_2 + \beta\gamma z}.$$

Substituting these equations into the last equation of (2.2) we arrive at

$$f(z) = \frac{\mu_3}{\nu}\frac{z}{y} = \frac{\beta\mu_3}{\nu}\frac{\mu_2 z + \gamma z^2}{\lambda\sigma\beta - \mu_1\mu_2 - \mu_1\gamma z} := h(z).$$

This allows us to demonstrate the number of solutions z^* as intersections of the graphs of $f(z)$ and $h(z)$ in Fig. 2. Algebraically, this equation is equivalent to $g(z) = 0$, where

$$g(z) = \beta\mu_3\gamma z^{n+1} + (\nu\mu_1\gamma + \beta\mu_2\mu_3)z^n - \nu(\lambda\sigma\beta - \mu_1\mu_2)z^{n-1} + a\beta\mu_3\gamma z + a\beta\mu_2\mu_3.$$

and the methods of single variable calculus can now be applied to complete the proof.

Theorem 2.2: Stability of P_0 and P_1

Part (1). Let $R_0 \leq 1$. Consider the Lyapunov function $V_0(x, y, z) = y$ for the equilibrium P_0 and differentiate along the differential equations (1.1). This yields

$$\begin{aligned}\dot{V}_0(x, y, z) &= \sigma\beta xy - \mu_2 y - \gamma yz \leq (\sigma\beta x - \mu_2)y \\ &\leq \left(\frac{\lambda\sigma\beta}{\mu_1} - \mu_2\right) y = (R_0 - 1)\mu_2 y \leq 0 \quad \text{if} \quad R_0 \leq 1.\end{aligned}$$

Here we have used the fact that $(x, y, z) \in \Gamma \implies x \leq \frac{\lambda}{\mu_1}$. Since the largest compact invariant set in $\{(x, y, z) \in \Gamma : \dot{V}_0(x, y, z) = 0\}$ is the singleton $\{P_0\}$, LaSalle's Invariance Principle gives that P_0 is globally asymptotically stable.

Part (2). Let $R_0 > 1$. Consider the Jacobian matrix of (1.1), $J(x, y, z)$.

$$J(x, y, z) = \begin{bmatrix} -\mu_1 - \beta y & -\beta x & 0 \\ \sigma\beta y & \sigma\beta x - \mu_2 - \gamma z & -\gamma y \\ 0 & \frac{vz^n}{z^n+a} & \frac{anvyz^{n-1}}{(z^n+a)^2} - \mu_3 \end{bmatrix}.$$

Therefore, at P_0,

$$J(P_0) = \begin{bmatrix} -\mu_1 & -\beta\tilde{x} & 0 \\ 0 & \sigma\beta\tilde{x} - \mu_2 & 0 \\ 0 & 0 & -\mu_3 \end{bmatrix}.$$

The eigenvalues of $J(P_0)$ are $-\mu_1$, $\sigma\beta\tilde{x} - \mu_2$, and $-\mu_3$. Thus, P_0 is unstable because

$$\sigma\beta\tilde{x} - \mu_2 = \mu_2(R_0 - 1) > 0.$$

At P_1,

$$J(P_1) = \begin{bmatrix} -\mu_1 - \beta\bar{y} & -\beta\bar{x} & 0 \\ \sigma\beta\bar{y} & 0 & -\gamma\bar{y} \\ 0 & 0 & -\mu_3 \end{bmatrix}.$$

The trace, determinant, and sum of 2×2 principal minors of $J(P_1)$ can be calculated as, respectively,

$$\begin{aligned} \mathrm{tr}(J(P_1)) &= -(\mu_1 + \mu_3 + \beta\bar{y}) < 0, \\ \det(J(P_1)) &= -\sigma\beta^2\mu_3\bar{x}\bar{y} < 0, \quad \text{and} \\ \mathcal{M}(J(P_1)) &= \sigma\beta^2\bar{x}\bar{y} + \mu_1\mu_3 + \beta\mu_3\bar{y}. \end{aligned}$$

Observe that

$$[\mathcal{M} \cdot \mathrm{tr} - \det](J(P_1)) = -(\mu_1 + \beta\bar{y})(\sigma\beta^2\bar{x}\bar{y} + \mu_1\mu_3 + \beta\mu_3\bar{y}) < 0.$$

Routh–Hurwitz conditions imply that P_1 is locally asymptotically stable. □

References

Asquith B, Bangham CRM (2007) Quantifying HTLV-I dynamics. Immunol Cell Biol 85:280–286
Bangham CR (2000) The immune response to HTLV-I. Curr Opin Immunol 12(4):397–402
Bangham CR (2003) The immune control and cell-to-cell spread of human T-lymphotropic virus type 1. J Gen Virol 84:3177–3189
Coffin JM, Hughes SH, Varmus HE (1997) Retroviruses. Cold Spring Harbor Laboratory Press, Cold Spring Harbor

Feldmann J, Schwartz O (2010) HIV-1 virological synapse: live imaging of transmission. Viruses 2: 1666–1680

Gallo RC (2005) History of the discoveries of the first human retroviruses: HTLV-1 and HTLV-2. Oncogene 24:5926–5930

Gomez-Acevedo H, Li MY (2002) Global dynamics of a mathematical model for HTLV-I infection of T cells. Can Appl Math Q 10:71–86

Gomez-Acevedo H, Li MY (2005) Backward bifurcation in a model for HTLV-I infection of $CD4^+$ T cells. Bull Math Biol 67:101–114

Gomez-Acevedo H, Li MY, Jacobson S (2010) Multi-stability in a model for CTL response to HTLV-I infection and its consequences in HAM/TSP development and prevention. Bull Math Biol 72: 681–696

Gout O, Baulac M et al (1990) Medical intelligence: rapid development of myelopathy after HTVL-I infections acquired by transfusion during cardiac transplantation. N Engl J Med 322:383–388

Greten TF, Slansky JE et al (1998) Direct visualization of antigen-specific T cells: HTLV-I Tax 11-19-specific $CD8^+$ cells are activated in peripheral blood and accumulate in cerebrospinal fluid from HAM/TSP patients. Proc Natl Acad Sci USA 95:7568–7573

Hollsberg P, Hafler D (1993) Pathogenesis of diseases induced by human lymphotropic virus type I infection. N Engl J Med 328:1173–1182

Hübner W, McNerney GP et al (2009) Quantitative 3D video microscopy of HIV transfer across T cell virological synapses. Science 323:1743–1747

Iwami S, Takeuchi Y et al (2007) Dynamical properties of autoimmune disease models: tolerance, flare-up, dormancy. J Theor Biol 246:646–659

Jacobson S (2002) Immunopathogenesis of human T cell lymphotropic virus type I-associated neurologic disease. J Infect Dis 186:S187–S192

Kato H, Koya Y et al (1998) Oral administration of human T-cell leukemia virus type 1 induces immune unresponsiveness with persistent infection in adult rats. J Virol 72:7289–7293

Kubota R, Osame M, Jacobson S (2000) Retrovirus: human T-cell lymphotropic virus type I-associated diseases and immune dysfunction. In: Cunningham MW, Fujinami RS (eds) Effects of microbes on the immune system. Lippincott Williams & Wilkins, Philadelphia, pp 349–371

Leroux C, Cadore JL, Montelaro RC (2004) Equine infectious anemia virus (EIAV): what has HIV's country cousin got to tell us? Vet Res 35:485–512

Nowak MA, May RM (2000) Virus dynamics: mathematical principles of immunology and virology. Oxford University Press, Oxford

Oh U, Jacobson S (2008) Treatment of HTLV-I-associated myelopathy/tropical spastic paraparesis: toward rational targeted therapy. Neurol Clin 26:781–797

Okochi K, Sato H, Hinuma Y (1984) A retrospective study on transmission of adult T-cell leukemia virus by blood transfusion: seroconversion in recipients. Vox Sang 46:245–253

Osame M, Janssen R et al (1990) Nationwide survey of HTLV-I-associated myelopathy in Japan: association with blood transfusion. Ann Neurol 28:50–56

Richardson JH, Edwards AJ et al (1990) In vivo cellular tropism of human T-cell leukemia virus type 1. J Virol 64:5682–5687

Seto K, Abe M et al (1995) A rat model of HTLV-I infection: development of chronic progressive myeloneuropathy in seropositive WKAH rats and related apoptosis. Acta Neuropathol 89:483–490

Wattel E, Cavrois M et al (1996) Clonal expansion of infected cells: a way of life for HTLV-I. J Acquir Immune Defic Syndr Hum Retrovirol 13:S92–S99

Wodarz D, Bangham CRM (2000) Evolutionary dynamics of HTLV-I. J Mol Evol 50:448–455

Wodarz D, Nowak MA, Bangham CRM (1999) The dynamics of HTLV-I and the CTL response. Immunol Today 20:220–227